Lidars for vehicles: from the requirements to the technical evaluation

Zhuoqun Dai[1*], Yang Li[2], Max Caspar Sundermeier[1], Tobias Grabe[1,4], Roland Lachmayer[1,3,4]
[1]Institute of Product Development, Leibniz University Hannover, Hannover, Germany
[2]Chengdu Pulse Optical Co. Ltd, Chengdu, P.R.China
[3]Cluster of Excellence PhoenixD, Leibniz University Hannover, Hannover, Germany
[4]GROTESK, Leibniz University Hannover, Hannover, Germany
*Contact email address: dai@ipeg.uni-hannover.de

Abstract— ADAS (Advanced Driver Assistance Systems) is a collective term of vehicle mounted sensors and devices aiming to improve traffic safety and realize high-level autonomous driving. Lidar systems are considered an indispensable part of ADAS to complement the other sensors like cameras and Radar. They realize these complements by providing a real-time high-resolution 3D representation of the environment of the vehicle, in which the positional information of each object area is included so that obstacles and potential hazards can be detected in advance by the ADAS. For this purpose, a Lidar must have the reliability of continuous work and provide the information accurately. In this paper, the requirements of Lidar systems in ADAS are firstly figured out by comparing them with other sensors applied in vehicles. Afterward, different types of Lidar systems regarding traffic safety and driver assistance are presented according to the stated Lidar function and driving condition on the road. Apart from the requirements, different working principles of Lidar products on the market are reviewed according to their scanning methods. Furthermore the results of this review are summed up in a technical evaluation to show the applicability of specific Lidar designs with respect to the requirements of vehicle applications.

Keywords: ADAS; autonomous driving; Lidar; requirements; review; technical evaluation

I. INTRODUCTION

Lidar is the acronym of "light detection and ranging". It emits a beam of light and measures the flight time of the light (TOF) to obtain the target range information. In 2004, the first Defense Advanced Research Projects Agency (DARPA) Grand Challenge for autonomous driving was held. None of the 15 participating autonomous vehicles completed the 142 miles desert course. A year later, a self-driving vehicle from Stanford University equipped with five SICK LMS-291 two-dimensional Lidars won the competition [1]. In 2007, the first 64-line Lidar was developed by Velodyne. In the DARPA Grand Challenge of the same year, five of the six finished vehicles were equipped with the Velodyne Lidar systems [2].

The past decade has seen a rapid development of Lidar sensors in automobile industry. However, one of the main obstacles to restrict their development is that few standards are formulated for Lidar sensors. In contrast, various standards and regulations are available for automotive lighting, e.g., UNECE vehicle regulation 8 for halogen headlamps and UNECE vehicle regulation 112 for LED headlamps [3] [4]. Therefore, the metrics of Lidar sensors are required to be investigated to further improve their performance. This paper provides an overview of important metrics of Lidar sensors and analyses the relationship between them. Chapter II introduces the ADAS functions and different levels in autonomous driving. In chapter III, a comparison of electromagnetic sensors applied on vehicles is presented. Subsequently, essential metrics of Lidar sensors are investigated in chapter IV. Chapter V analyses the requirements of laser safety and discusses the influence of weather conditions. Consequently a technical evaluation of different vehicle-mounted Lidar systems is provided.

II. ADAS AND AUTONOMOUS DRIVING

Advanced Driver Assistance Systems (ADAS), as the name describes, help drivers avoid accidents by supporting different driving tasks [5]. The driving tasks of interest for ADAS can be divided into two different categories: Lateral controls and longitudinal controls. In Table I the fundamental driving tasks of ADAS are listed.

TABLE I. REVIEW OF DRIVING TASKS OF ADAS ACCORDING TO [5]

Lateral Controls	*Longitudinal Controls*
• Lane Departure Warning (LDW) • Blind Spot Detection (BSD) • Lane Change Asistance (LCA)	• Adaptive Cruise Control (ACC) • Forward Collision Warning (FCW) • Emergency Brake Assist (EBA) • Forward Crash Mitigation (FCM) • Traffic Sign Recognition (TSR)

According to the SAE Standard J 3016 autonomous driving is divided into six levels regarding the extent of which the vehicle replaces the driver to perform driving tasks. Level 0 stands for no automation so that the driver has to perform all the driving tasks, while the vehicle has to perform all the driving tasks by full automation in Level 5 [6]. The functions of ADAS are corresponding to different levels in autonomous driving. For instance, LDW and BSD are categorized as Level 0 because they only provide the driver visual and auditory cues. Instead, the driver requires to control the vehicle completely. In contrast, ACC adjusts the speed of the vehicle to ensure a safe distance from the vehicle ahead, hence can be classified as Level 1 [7]. To support the driving tasks mentioned in Table I, four major sensors are integrated on the vehicle, namely ultrasonic sensors, cameras, Lidar and radar. Ultrasonic sensors measure the flight time of an ultrasonic pulse to obtain the distance information [8]. Due to the limitation of sound speed, ultrasonic sensors are generally applied for low-speed driving conditions. Compared to ultrasonic sensors, cameras, Lidar and radar are based on electromagnetic waves. Therefore, the target can be detected in real-time at a high driving speed. The sensor fusion can take advantage of different sensors and improve system reliability. Hence, to investigate strengths and weaknesses of cameras, radar and Lidar, their principles will be investigated in the next chapter.

III. ELECTROMAGNETIC SENSORS

Electromagnetic sensors measure the required physical quantities by actively transmitting or passively receiving electromagnetic waves converting the electromagnetic signals into electrical signals. Among them, vehicle-mounted optical sensors usually utilize wavelengths in the visible, infrared and radio spectrum to measure objects (Fig. 1).

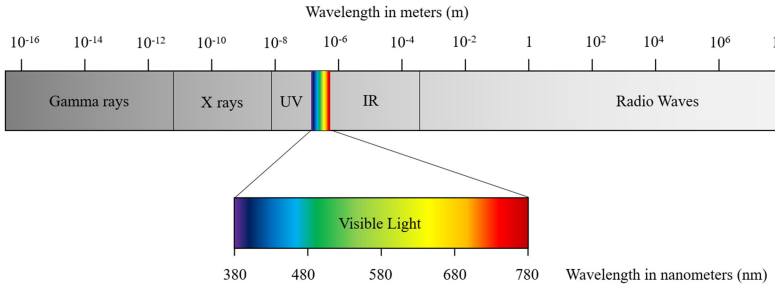

Figure 1. Electromagnetic spectrum according to [9]

A. Camera

Cameras are generally classified as passive sensors that typically use a charge-coupled device (CCD) and a complementary metal oxide semiconductor (CMOS) as detector. Due to their high quantum efficiency in the visible spectrum (380 nm to 780 nm), cameras can provide high-resolution chromatic images. Thus, their main task in autonomous driving is to identify and track objects [10]. Compared to CCD sensors, the compactness, low mass, low power consumption and radiation tolerance gives CMOS sensors advantages. However, CCD sensors offer advantages in dynamic range and photometric accuracy [11].

TOF-cameras illuminate the pulsed light to a desired field of view (FOV). The distance (D) is measured with the fight time of the transmitted pulse T_{TOF} and the light velocity c. The distance of the measurement is expressed in (1) [11].

$$D = c \cdot T_{TOF}/2 \tag{1}$$

The distance (D) is proportional to the flight time of the pulse T_{TOF}, whereby light propagates with the constant speed (c). In addition, stereo cameras also provide depth images while providing chromatic information using the principle of triangulation ranging. However, due to the energy being emitted in a wide FOV and the decreasing

accuracy of triangulation for increasing distance, the detection range of both TOF systems and stereo camera is limited. Since the detectors of most cameras are sensitive for visible light, the signal quality strongly depends on ambient light and weather conditions. In most actual automatic driving schemes, cameras are accordingly fused with Lidar sensors in order to improve the identification accuracy and system reliability [12] [13].

B. Radar

Radars use millimeter-waves to measure the radial distance and the velocity of a mobile target with high precision. In addition, they are also robust under extreme environmental conditions, e.g. low illumination, snow and rain [14]. Compared to cameras and Lidar, radar systems measure the relative velocity of a target directly using the Doppler Effect. The two typical frequencies for automotive radar sensors are 24 GHz and 77 GHz. Compared to 77 GHz radars, 24 GHz radars are developed for short range applications and have the advantage of low cost and small size. To measure the angular positions of a target, several units have to be adjacently arranged. 77 GHz radar sensors are mainly used for long range detection to realize ACC and EBA in ADAS [15]. Compared to 24 GHz sensors, 77 GHz radars require a smaller antenna aperture, which refers to a smaller size of the sensor. Additionally, the benefit of a high operating frequency is a reasonable spatial resolution due to the combination of both high transmitted power and narrow modulated pulse width [16]. One of the main drawbacks of radar sensors compared to cameras is their lack of angular resolution. Therefore, they also require to be fused with other sensors to recognize more details of objects.

C. Lidar

Lidars are optical sensors that utilize near infrared radiation and are usually composed of emitter, detector, beam steering devices and a time-to-digital converter circuit (TDC) to determine distance information [17]. The coverage of the FOV is achieved by optical lenses or scanning devices. For vehicle-mounted Lidars, the principle of distance measurement is based on TOF and can be divided into two modes. In direct TOF, the time difference between the transmitted pulse and the received signal is measured [18]. Assuming that the emitter and the detector are at the same position, a laser pulse travels along the path to the reflecting object twice within the TOF. In indirect TOF, a continuous modulated sinusoidal wave (cw) is transmitted. The phase difference between the transmitted signal and the received signal is measured [19]. The main tasks of Lidar sensors in autonomous driving are odometry and mapping [20]. Moreover, Lidars can also be used for lane detection due to the measurement of different object reflectivity in a point cloud [21]. The Audi A8 was the first commercial vehicle equipped with a Lidar system for ACC to help the driver steer, accelerate and brake [22]. The further performance metrics of Lidar sensors are investigated and discussed in detail in the next chapter.

According to the reviews in this chapter, the advantages and disadvantages of electromagnetic sensors are summarized in Table II. Due to the sensitivity for visible light, cameras are able to provide not only grayscale images, but also chromatic information, which is necessary to detect the signal lamps. Lidar sensors provide a large FOV and measure the distance of objects precisely and independent of the ambient lighting conditions.

TABLE II. ADVANTAGES AND DISADVANTAGES OF OPTICAL SENSORS

Sensors	***Advantages***	***Disadvantages***
Cameras	+ Chromatic information + Very high resolution + Object detection/classification	– Limited range detection – Low robustness in poor lighting and weather conditions
Radar	+ Robustness against poor weather conditions + Independence of lighting conditions + Measurement of velocity	– Low angular resolution – Recognition of color
Lidar	+ Large FOV + Independence of lighting conditions + Accurate range measurement + High resolution	– Recognition of color – Vulnerability of mechanical scanning components

IV. PERFORMANCE METRICS OF LIDAR SYSTEMS

In this chapter the important metrics of Lidar sensors are analyzed based on exemplary commercial devices.

A. Wavelength of Emitter

The wavelength of the emitter is an important parameter of Lidar sensors. It determines the sensitivity of the photodiodes used as detectors, has a significant impact on laser safety aspects (section G) and on the atmospheric absorption (section 5C). As previously described Lidar sensors operate in the near infrared spectrum (780 nm to

3000 nm). To generate laser beams in the corresponding spectrum, two types of laser diodes are typically applied in Lidar systems.

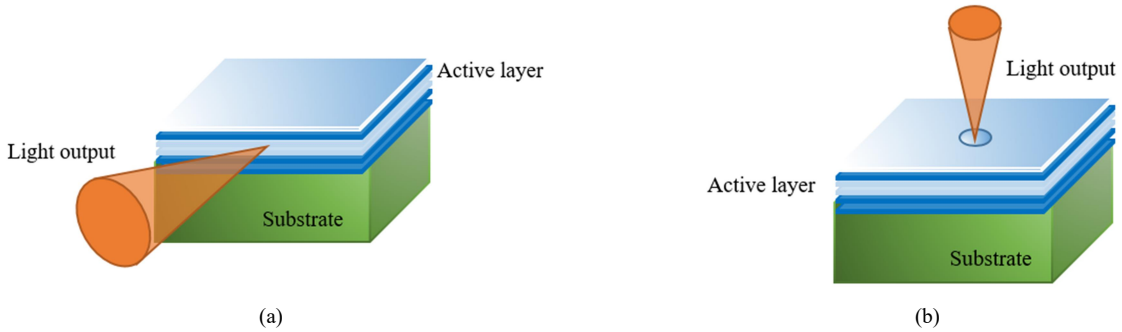

Figure 2.The structures of laser diodes. (a) Edge-emitting laser. (b) Vertical-cavity surface emitting laser according to [23]

Fig. 2 indicates the basics structure of both edge-emitting lasers (EELs) and vertical-cavity surface-emitting lasers (VCSELs). Compared to VCSELs, the advantage of EELs is the high emission power. In the case of a constant background noise this leads to a good signal-to-noise ratio (SNR) and helps to achieve a large detection range. Lidar sensors utilize bandpass filters to reflect background noise such as sunlight and head lamp radiation. A wavelength-specific grating is built into the active layer of VCSELs that reduces the wavelength shift with temperature down to 0.07 nm/°C. Hence, VCSELs have a narrow wavelength range of the emission and can be equipped with a narrow bandpass filter to reduce noise reaching the detector [24]. Since the emitted beam shows a circular cross section, beam shaping for VCSELs is relatively easy. In practice, since limited in output power, VCSELs are more appropriate for Lidar systems that are used for short range ADAS functions, e.g. blind-spot detection (BSD), lane departure warning (LDW) and rear cross traffic alert (LCA) [24].

Most commercial Lidar systems are based on a wavelength of 905 nm or 1550 nm. Avalanche photodiode detectors (APD) are silicon-based photo detectors used for Lidar systems due to their high photoelectric conversion rate of at least 80% for 905 nm. For Lidars with a wavelength of 1550 nm, indium gallium arsenide (InGaAs) photodiode detectors are designed to detect this wavelength [25].

B. Field of View

The field of view refers to the angular coverage of a Lidar frame and is expressed by the horizontal field of view (FOV_H) and vertical field of view (FOV_V). Mechanical spinning Lidars are able to generate a 2π radian horizontal coverage. For scanning Lidars, the FOV is defined under the consideration of the refresh rate and the interval between two adjacent pulses. In other words, the system must scan the total FOV within one frame. The FOV of flash Lidars is determined by the lens system used [26].

The FOV_V refers to the coverage of the object height in a certain distance. As an example, for a full coverage of objects with a height of 1.5m in a short range of 0.5 m, a minimal FOV_V of 70° is required, which refers to an essential metric for short range Lidars with the detection range < 50 m. For long range Lidar systems the same target height in 200 m is able to be fully covered with only a 0.9° FOV_V. Therefore, the design of FOV_V is based on the coverage requirements of different object heights at different distances. In general, the FOV_V of short range Lidars is larger than that of long range Lidars.

The requirements for FOV_H can be determined by the applications in ADAS or autonomous driving. ADAS applications such as blind spot detection (BSD), traffic sign assist (TSA) and rear cross traffic alert (RCTA) require to monitor an angle of 120° near the vehicle [5]. Further applications of ADAS such as adaptive cruise control (ACC) and emergency break assist (EBA) are focused on the area in front of the vehicle with a FOV_H of 25° but a long distance of over 150 m [5]. In full autonomous driving the monitoring of the entire surrounding environment (360° FOV_H) is necessary [27].

C. Maximum Detection Range

The maximum detection range of Lidars is defined as the distance in which the reflection of a Lambertian scatterer with a reflectivity of 10% can still be detected [28]. The frequency of the emitted pulse limits the detection range as well. Since emitter and detector are time-synchronized, the reflection of the first pulse must be detected before emitting the next one (Fig. 3).

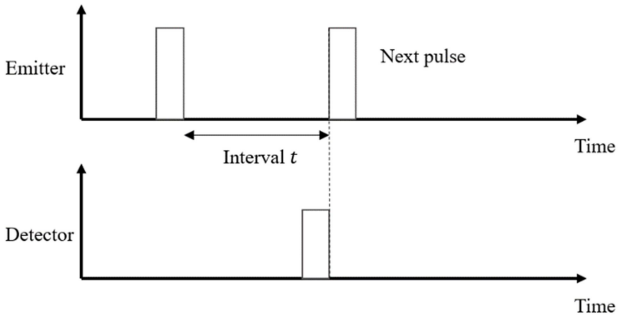

Figure 3. Pulse modulation at the emitter and detector

The calculation of the theoretical maximum detection range of a pulsed Lidar is given in (2).

$$R_t = c \cdot t/2 \tag{2}$$

R_t is the theoretical maximum detection range, c is the speed of light in air and t is the pulse interval. For a maximum detection range of 500 m, the transmitted pulse has to be modulated with less than 300 kHz. In practice, the detection range of Lidars is often affected by the output power of the emitter (P_T), the transmission efficiency of the optical system (η_{sys}) and the atmospheric attenuation (η_{atom}). Hence, the practical maximum detection range R_p can be expressed by (3) [29].

$$R_p = \eta_{atom} \sqrt{P_T \cdot \varepsilon \cdot A_{rec} \cdot \eta_{sys} / (A_{illum} \cdot \pi \cdot P_R)} \tag{3}$$

P_R is the received power of the detector. ε is the cross-sectional illuminated area of an object. A_{illum} is the area illuminated of an object. A_{rec} is the area of the receiver. According to (3), the detection range can be increased by increasing the output power or the transmission efficiency in the atmosphere. Therefore, these two parameters will be discussed in detail in chapter V. Besides them, other influencing factors are the characteristics of a detected object and the optical system of Lidar systems. While the first cannot be influenced by the Lidar system designer, the second offers a wide area of research that cannot be covered in this paper.

D. Distance Resolution

The distance resolution ΔR refers to the ability of a Lidar system to distinguish a distance separation between two targets, which is mainly determined by sampling frequency of the TDC (B) and can be expressed in (4) [30].

$$\Delta R = c/2B \tag{4}$$

As examples, analog front-end (AFE) circuits developed for linear-array detectors in [31] and [32] have the sampling frequencies of 450 MHz and 1200 MHz respectively, which means the range resolution can reach an order of a decimeter. For a range resolution in order of a centimeter a minimal sampling frequency of 1.5 GHz is required.

E. Angular Resolution

The angular resolution is defined by the minimum angular distance between two objects which can be resolved by a Lidar system [33]. It refers to the corresponding angle between two adjacent scanning points or two neighbor pixels on detectors. Level 4 autonomous driving requires an angular resolution of 0.1° x 0.1° [28]. In terms of the requirement, a detected object in 200 m is roughly 35 x 35 cm in dimension.

F. Laser Safety

Standard IEC 60825-1 ranks the safety of laser products in the wavelength range 180 nm to 1 mm with eight levels from Class 1 to Class 4 according to the increase of ocular hazard. Class 1 laser safety refers to laser products that are safe for long-term intrabeam viewing. In particular, “eye safe” describes only Class 1 products [34]. Since vehicle-mounted Lidar systems must be “eye safe”, they have to fulfil the Class 1.

According to the structure of human eyes, light has to pass the cornea, aqueous humor, lens and vitreous humor to reach the retina. These structures are transparent to radiation with a wavelength between 400 nm and 1400 nm. Therefore, Lidars with a wavelength less than 1400 nm can be dangerous for human eyes and hurt the retina. For wavelengths from 1500 nm to 2600 nm, the heat effect is able to dissipate over the greater volume of aqueous humor.

Therefore, Lidars with a wavelength of 1550 nm can provide a greater output power without increasing the risk for the human eye. According to the standard IEC 60821-1, the evaluation of the laser safety is not only related to the output power and wavelength of a laser source, but also related to other metrics of the system, e.g., pulse width, pulse frequency and divergence of the laser beam.

G. The Type of Lidar Systems

Lidar sensors can be divided into three types based on their beam steering method. Lidars with a rotating emitter and detector can be regarded as mechanical Lidar. In hybrid solid state Lidars emitter and detector are not moved. Instead the steering of the beams is realized by movable optical components, such as micro-electro-mechanical systems (MEMS) and Risley prisms. Solid state Lidars illuminate the total FOV as so-called flash Lidar systems or utilize phased-array optics (OPA) to steer beams. Fig. 4 discloses the different scanning methods of Lidar sensors.

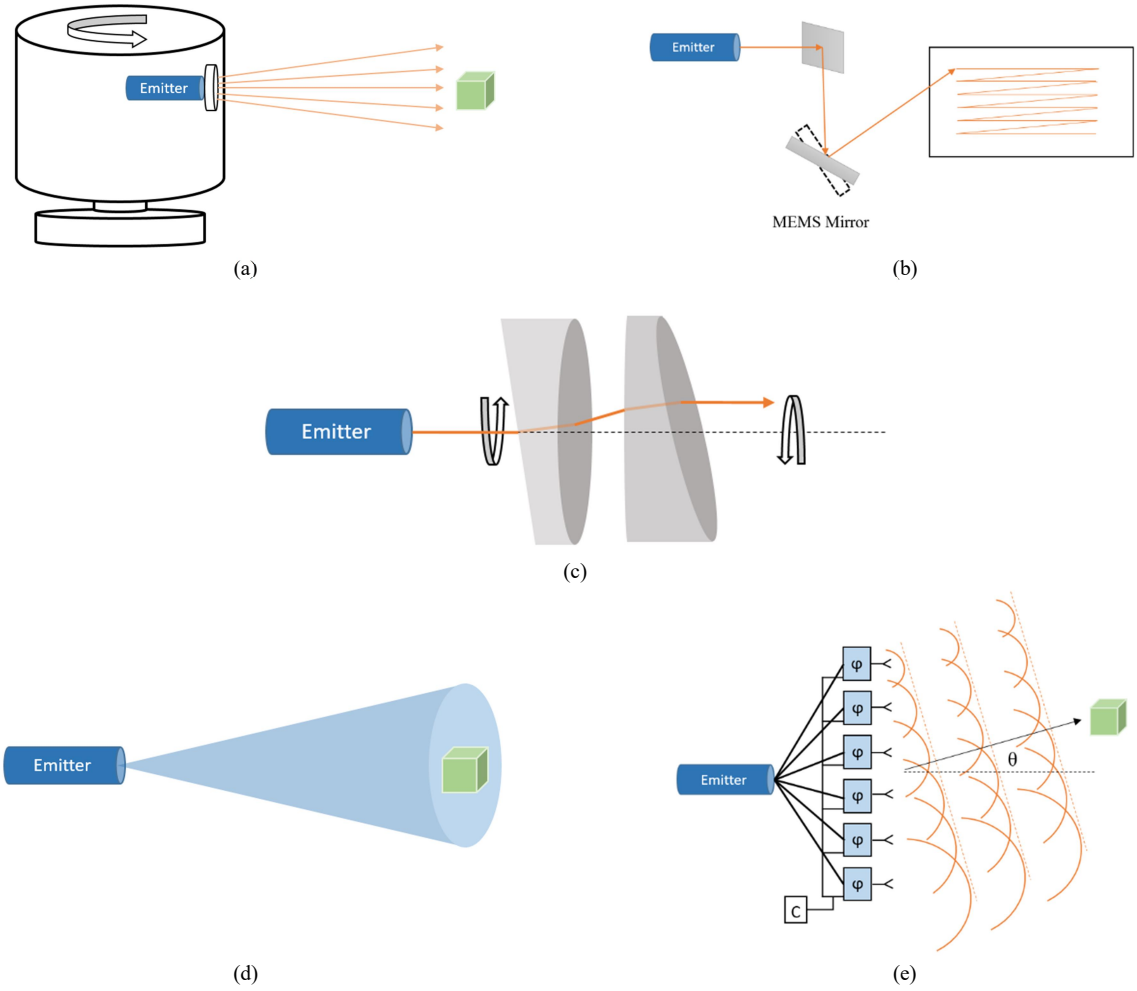

Figure 4. (a) Spinning scanner in mechanical Lidar. (b) MEMS scanning method. (c) Risley prism scanning. (d) Flash illumination. (e) OPA beam steering

Mechanical spinning Lidars integrate a stack of photodetectors to scan a target in several horizontal layers. Both emitters and detectors are motorized and rotate with an angle of 360° (Fig. 4a) to generate a 2π radian FOV_H. Moreover, due to the use of moveable parts, such systems are less tolerant against such as mechanical vibrations compared to other Lidar systems. Therefore, the system vulnerability needs to be considered in practical applications. Further, specific requirements for the electric power are to be considered for the rotating parts. Manufacturers of mechanical Lidars are for example Velodyne, Hesia, Ouster and Robosense.

As a compromise of the benefits of mechanical systems and a robust setup, MEMS scanning systems as shown in Fig. 4b not only provide a wide FOV, but also micro-motion units, which improves their reliability. Additionally, MEMS devices have been successfully applied to technologies of projectors and displays [35] [36]. Digital micromirror devices (DMD) are possible to generate a high-resolution light distributions in automotive lighting to improve the driving safety [37] [38]. In addition to switching the light, they are also able to modulate the phase of the incident light to steer beams and generate holographic projections [39] [40]. Manufacturers of MEMS Lidars are for example Aeye, Blickfeld, Hesai, Innoviz, Robosense, Luminar and LeiShen.

Fig. 4c indicates the principle of Risley prism scanners that utilize at least two sequential rotating wedge prisms to steer the beam [41]. The speed ratio of the two prisms determines the shape of the scanning area. The emitter is typically an array of laser diodes to increase the scanning density in the FOV. For example, a Lidar based on Risley prisms is Livox Horizon which scans a close-to-rectangle FOV using three rotating prisms. The first two prisms rotate with the same speed in opposite directions, while the third prism rotates simultaneously with a lower speed [42]. Lidar systems that utilize the mechanical spinning methods, MEMS and Risley prisms to steer beams are also named scanning Lidars. These systems often integrate an array of light sources to achieve a multi-beam scanning or to increase the scanning density. Correspondingly, the detector is also arranged as a linear array [43] [44] [45].

In contrast to scanning Lidars, flash Lidars illuminate the entire FOV at once using projecting lenses (Fig. 4d). A so-called focal plane array (FPA) is used to detect the reflections and measure the TOF for all pixels simultaneously [46]. The angular resolution is determined by the density of pixels on the detector. In order to detect the reflection signals with a larger number of pixels on the detector, a greater laser pulse energy is needed. According to (3), a larger cross-sectional area of the transmitted beams can decrease the detection range. Hence, flash Lidars are mainly designed for near range detection [47]. Compared to scanning Lidars, the detector of flash Lidars is arranged in a matrix form [48]. LeddarTech, Ibeo, Continental, Ouster and Cepton are exemplary manufacturers of flash Lidars.

Optical phased arrays (OPA) are a beam steering technology to avoid movable parts in Lidar systems. This technology was firstly used for radio waves to steer and control the beam direction using phase delay and interference between antennas [49]. The laser beam in Fig 4e is split to several phase shifters to modify the phasing of the output wave front and control its direction. One of the challenges of OPA technology is reducing the grating side lobes to increase the FOV_H [50]. Using OPA technology for radio waves has proved that the element spacing of antenna arrays has to be less than the half of the operating wavelength [51]. Under this condition the grating side lobes are can be reduced, so that scanning the entire FOV with the main lobes is possible. For Lidar systems using wavelengths in the spectrum with an order of one micrometer, it increases the difficulty of antenna processing undoubtedly. As far as known, Quanergy is the single manufacturer of OPA Lidars.

V. DISCUSSION

A. Scanning technologies

As mentioned in section C chapter IV, the emitted power and the transmission of laser beams in the atmosphere are two parameters that determine the maximum detection range of a Lidar system according to (3). Hence, the influence of these two parameters will be discussed in this chapter. Fig. 5 indicates a comparison of Lidar Systems with diverging illumination and collimated beam respectively.

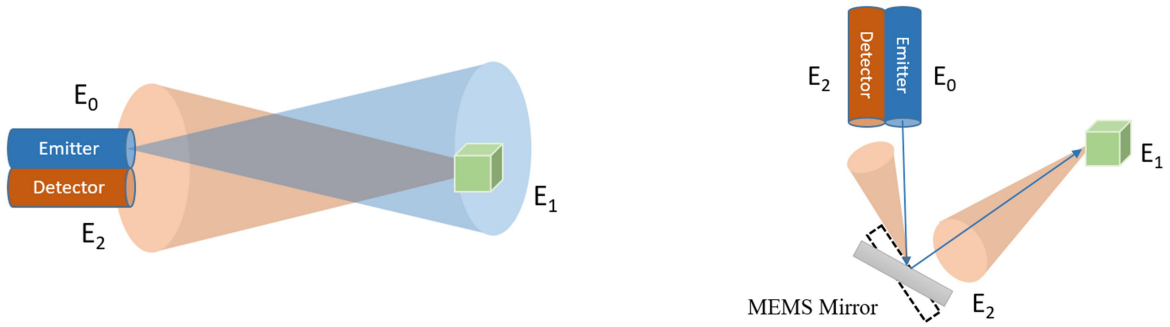

Figure 5. (a) Lidar with diverging illumination. (b) Lidar with collimated beam

As previously in (3) described, the energy ratio of the output energy and received energy is proportional to the square of the target distance. Assuming the output energy of the emitter E_0, the energy E_1 that reaches the target and the energy E_2 reaches the detector, for the system in Fig. 5a the returned energy E_2 is given by $E_2 \propto (1/R^2)E_1 = (1/R^4)E_0$ [29]. For a scanning Lidar with a theoretically perfectly collimated beam, the energy E_1 reaching the target would not depend on the distance and is therefore expressed by $E_1 \propto E_0$ [29]. Furthermore the returned energy E2 is given by $E_2 \propto (1/R^2)\ E_0$ (Fig. 5b). In addition, a Lidar with collimated beams has significantly small area illuminated of an object (A_{illum}) to detect further according to (3). Consequently, for scenes with a constant background noise, Lidar systems with a collimated beam are able to reach an increased detection range [52]. According to section G chapter IV, a collimated beam is available in mechanical spinning Lidars, MEMS Lidars and Risley prism Lidars.

B. Output Power based on Laser Safety

As discussed in section C chapter IV the detection range of a Lidar system can easily be increased by enlarging the output power. However, this parameter is limited by the requirements of laser safety. Hence, laser safety for different modulations and wavelengths has to be investigated. As mentioned in section G chapter IV, all the vehicle-mounted Lidar systems have to fulfill laser safety Class 1. The flow chart in Fig. 6 is designed to calculate the maximum accessible transmitted power of a Lidar system [34].

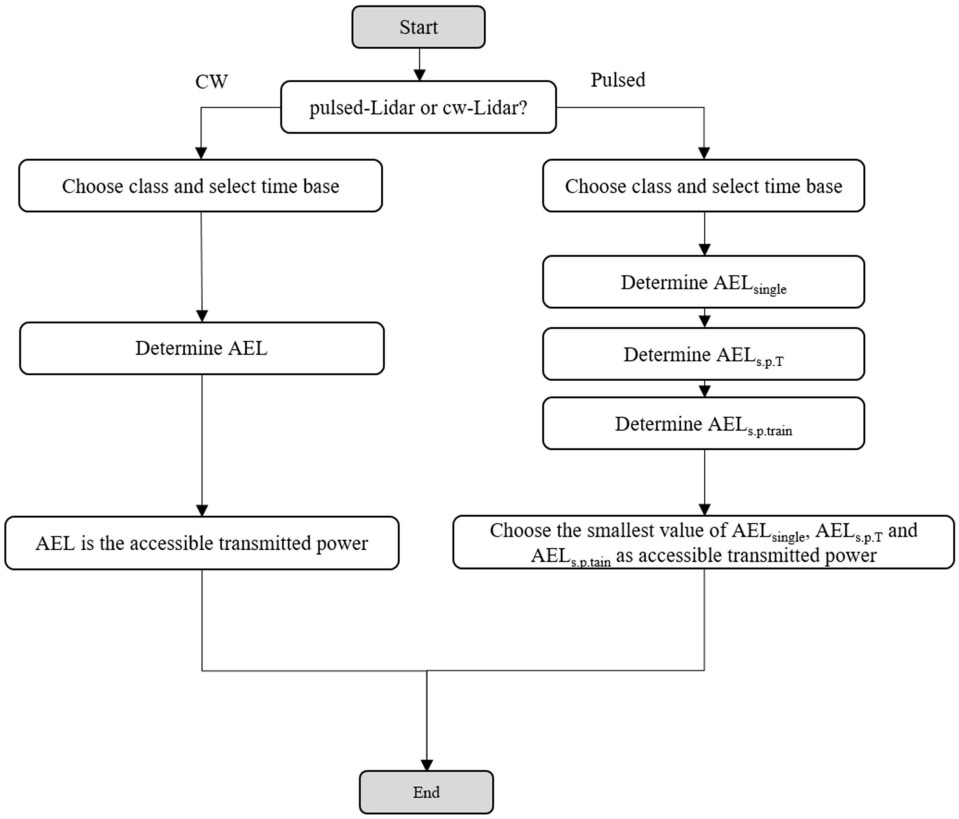

Figure 6. Flow chart to calculate the maximum accessible output power of a pulse Lidar simplified according to IEC 60825-1 [34]

According to the flow chart (Fig. 6), the evaluation of a cw-Lidar requires to determine the maximum accessible emission permitted (AEL) based on a table of accessible emission limits for Class 1 in IEC 60825-1. For all Class 1 laser products the time base has to be selected with 100 s. Assuming cw modulated Lidars with the laser safety Class 1, the maximum output power of the emitter with a wavelength of 905 nm is 3.00 mW and 10.00 mW.for 1550 nm respectively.

To evaluate a pulsed-Lidar, the accessible emission limit for a single pulse (AEL_{single}), the accessible emission limit for a single pulse based on duration T ($AEL_{s.p.T}$) and the accessible emission limit for a single pulse in the pulse train ($AEL_{s.p.train}$) have to be compared to find the most restrictive parameter. The maximum allowable output power for 905 nm and 1550 nm will be calculated separately, assuming the exemplary parameters of Table III.

TABLE III. THE ASSUMPTION OF LIDAR METRICS

Parameters of Lidar	***Value***
Wavelength	905 nm / 1550 nm
Pulse Width	2 ns
Pulse Frequency	40 kHz
Laser safety class	Class 1
Divergence of the Laser	Beam collimated: < 1.5 mrad

The assumption of 2 ns pulse width corresponds to a range resolution of 3 cm and is an average value of the investigated commercial Lidar products. The pulse repetition frequency refers to the theoretical maximum detection range and the number of Lidar points generated per second with a single return signal. To this end, the exemplary chosen pulse frequency of 40 kHz is an average value of the investigated products. The divergence angle of the laser indicates the scanning method of the system. For a scanning Lidar the laser beam is well collimated and can be assumed with a divergence angle of less than 1.5 mrad. For Lidar systems with diverging illumination, the standard IEC 60825-1 does not limit the peak output power for the wavelengths >1400 nm. Therefore, flash Lidars using 1550 nm wavelength have a significant advantage in terms of laser safety. For both modulation methods, the peak output power can be further increased by at least an order of magnitude while using 1550 nm as operation wavelength. Accordingly, pulse modulated Lidar systems with a wavelength of 1550 nm offer the highest peak output power in this comparison and therefore enable the largest detection range. The disadvantage of Lidar sensors with 1550 nm is the use of InGaAs photodetectors which require external cooling systems, cause additional costs and increase the required installation space [25].

C. Laser Beam Attenuation in the atmosphere

Another factor that influences the detection range of Lidar systems according to (3) is the transmission of laser beams in the atmosphere which is mainly determined by absorption and scattering by different gas components [53]. The absorption of the near infrared is mainly due to water (H_2O), ozone (O_3) and carbon dioxide (CO_2) [54]. The main forms of these three molecules in the atmosphere are H_2O^{16}, $O^{16}{}_3$ and $C^{12}O^{16}{}_2$, compared with their isotopes, their proportion are 99.73%, 99.40% and 98.42% respectively [53]. 90 to 95% of ozone is found in the stratosphere, nearly all of the remaining 5 to 10% is found in troposphere [55]. Hence the absorption of infrared radiation by ozone in ground level can be disregarded. Therefore, H_2O and CO_2 need to be analyzed regarding the absorption of the infrared essentially. Fig. 7 indicates the transmittance in the infrared between 5000 cm^{-1} (2000 nm) to 12820 cm^{-1} (780 nm) for molecules of water and carbon dioxide using HITRAN (High-resolution Transmission Molecular Absorption) database.

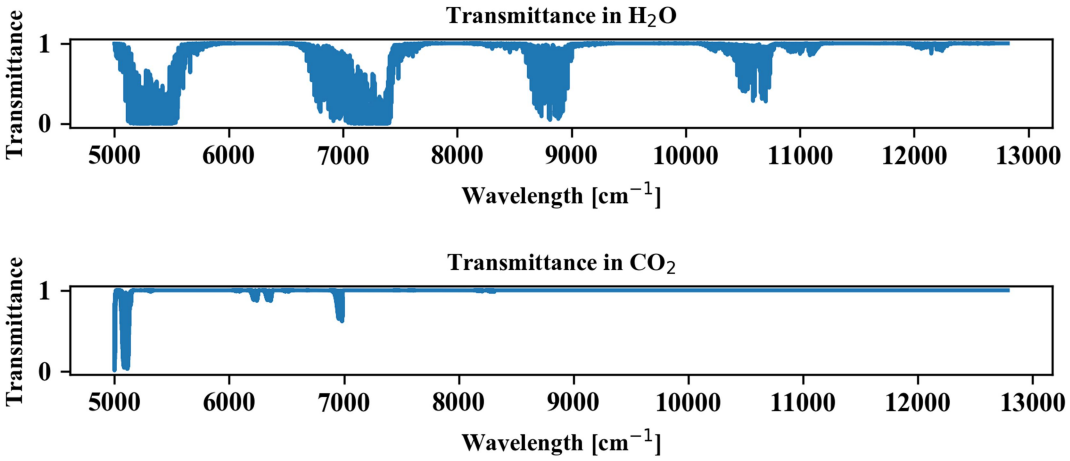

Figure 7. Transmittance of IR between 780 nm (12820 cm^{-1}) to 2000 nm (5000 cm^{-1}) in molecules of water and carbon dioxide based on HITRAN datebase according to [54]

The HITRAN data used in Fig. 7 are measured for a room temperature of 296 K and pressure of 1 bar [54]. Apparently, there are four absorption peaks for water molecules. Meanwhile, carbon dioxide molecules hardly absorb infrared in the corresponding range. Water molecules are by far the most important absorbing component in the atmosphere for near infrared. In order to compare its absorption for the two typical wavelengths used in Lidar systems, a high resolved section of the resolution transmittance curve of water is given in Fig. 8.

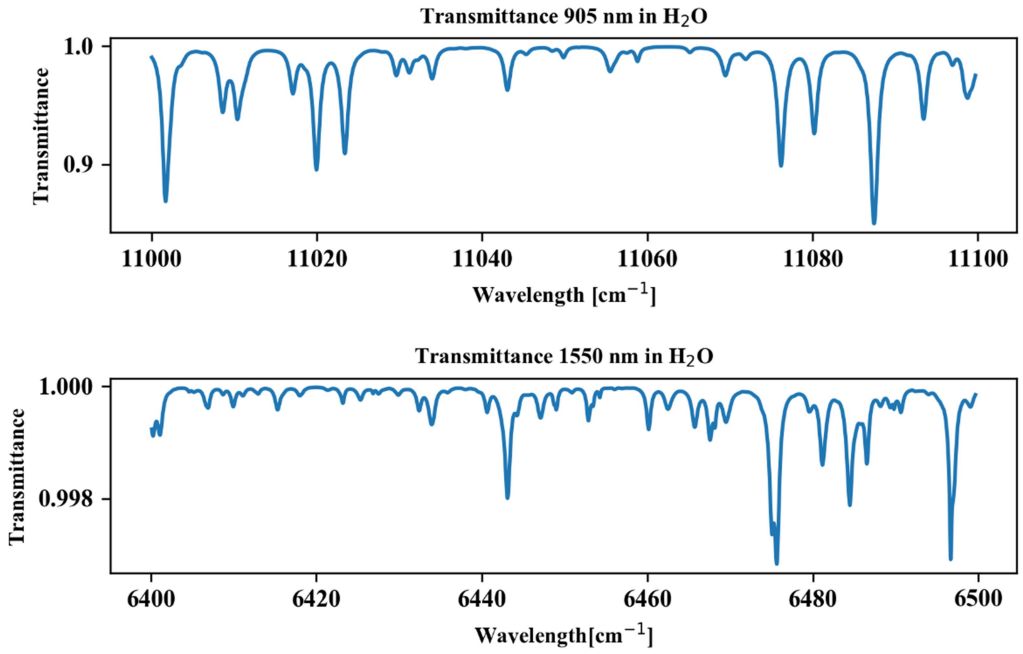

Figure 8. Transmittance of 905 nm (11050 cm^{-1}) and 1550 nm (6450 cm^{-1}) in water molecule according to the HITRAN database [54]

According to Fig. 8, the transmittance for 905 nm (11050 cm^{-1}) of water molecules is approximately 98% and above 99.9% for 1550 nm (6450 cm^{-1}). Moreover, the proportion of water vapor in the atmosphere is 0.1% to 1% of all molecules. Hence the absorption of atmospheric molecular contributes barely to the total attenuation [56]. For a more realistic evaluation the spectral width of the laser emission and the thermal shift of the central wavelength also have to be considered.

Since the molecular absorption has no significant effect on the atmosphere attenuation, the influence of scattering requires to be evaluated. Three types of scattering occur depending on the size of the scattering object. The size parameter α, which indicates the ratio of the particle size r in the atmosphere to the wavelength λ of the laser, determines the type of scattering [56].

$$\alpha = 2\pi r/\lambda \tag{5}$$

Table IV indicates the radius of typical particles in the atmosphere and the corresponding size parameter for laser with wavelengths of 905 nm and 1550 nm respectively [57] [58].

TABLE IV. RADIUS OF DIFFERENT SCATTERING PARTICLES AND CORRESPONDING SIZE PARAMTER FOR LASER WITH WAVELENGTH OF 905 NM AND 1550 NM ACCORDING TO [57] [58]

Type of Scattering	*Radius r [µm]*	*Size Parameter α*	
		905 nm	*1550 nm*
Air Molecules	0.0001	0.0007	0.0004
Haze particle	0.01 ~ 1	0.07 ~7	0.04 ~ 4
Fog	1 ~ 20	7 ~ 140	4 ~ 8
Rain	100 ~ 10000	700 ~ 70000	400 ~ 40000
Snow	1000 ~ 5000	7000 ~ 35000	4000 ~ 20000
Hail	5000 ~ 50000	35000 ~ 350000	20000 ~ 200000

Rayleigh scattering occurs for α <0.1. Mie scattering takes place for α in the region of 0.1 to 10. When the size of a particle is much larger than the transmitted wavelength (α > 10), geometrical scattering is dominant, which refers to the weather conditions of rain, snow and hail for the considered wavelengths (compare Table IV). Rayleigh and Mie scattering depend on the wavelength, geometrical scattering is independent of the wavelength of incident light [53]. Therefore, the influence of the wavelength on atmospheric attenuation for weather conditions like rain, snow and hail can be neglected [59].

An empirical equation in (6) describes the attenuation due to atmospheric Mie scattering under the rest of weather conditions in Table IV such as haze and fog [60].

$$\sigma = 3.91 \cdot V^{-1} (\lambda/550)^{-q} \tag{6}$$

Where σ is coefficient of atmospheric attenuation caused by scattering
V is visibility in km
λ is wavelength of emitter in nm
q is the distribution of the scattering particles and determined with different visibilities, and can be expressed by

= 1.6	for visibility V > 50 km
= 1.3	for visibility 6 km < V < 50 km
= 0.16 V + 0.34	for visibility 1 km < V < 6 km (haze)
= V – 0.5	for visibility 0.5 km < V < 1 km (mist)
= 0	for visibility < 0.5 km (fog)

Under the consideration of Beer-Lambert Law, the transmittance rate τ of a laser at a given range R can be expressed as $\tau(R) = \exp(-\sigma R)$. Based on this, the transmittance for the wavelengths 905 nm and 1550 nm at an exemplary distance of 200 m in dependence of the visibility is given in Fig. 9.

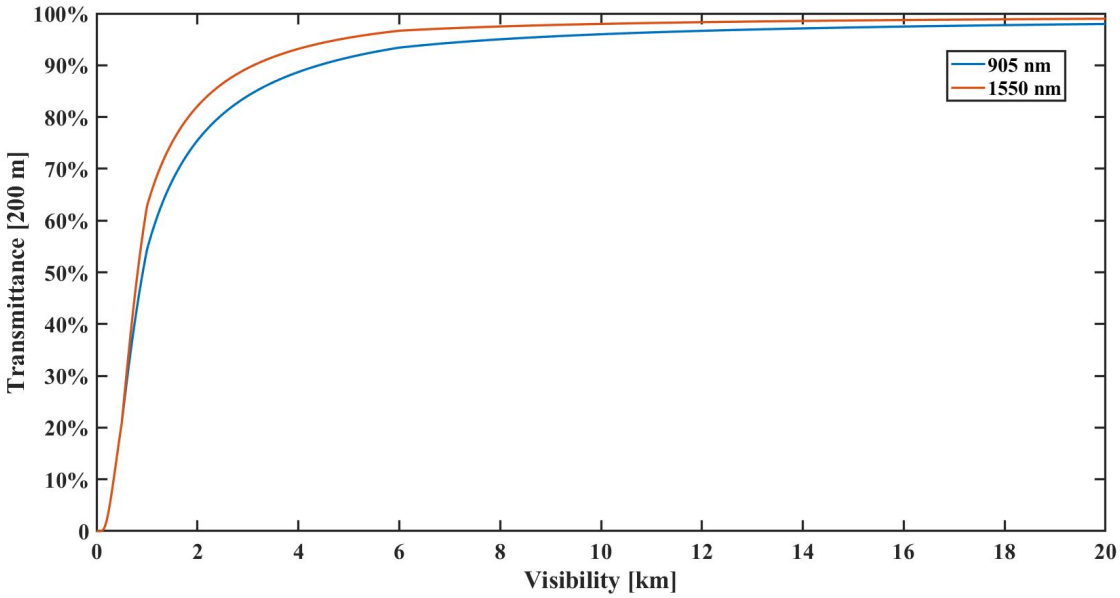

Figure 9. Transmittance for 905 nm and 1550 nm at 200 m under all-weather conditions (visibility)

According to the Fig. 9, no difference is indicated between the scattering losses at 1550 nm and 905 nm for typical fog conditions (< 0.5 km visibility). For larger visibility distance the wavelength 1550 nm indicates small advantages.

D. Technical evaluation of different Lidar systems

Since different types of Lidar systems are available on the market, it is necessary to evaluate their performance. Based on the investigation on important Lidar metrics in chapter IV and chapter V as well as on the data of commercial available Lidar systems, a technical evaluation is developed (Table V).

TABLE V. TECHNICAL EVALUATION OF LIDAR SYSTEMS

Beam steering methods	*Technologies*	*Reliability*	*FOV*	*Max. Detection Range*	*Angular Resolution*	*Laser Safety*
Scanning	Mechanical spinning	-	+++	++	++	++
	MEMS	++	++	+++	++	+++
	Risley Prism	++	++	++	++	++
	OPA	+++	-	++	+	++
Non-scanning	Flash	+++	+	-	-	++

Scala：Excellent + + +, Good + +, Average +, Fair -, Poor --

While the mechanical spinning Lidar can realize a 360° FOV_H with a single sensor, the reliability is in dispute due to moving parts. By contrast, the micro-motion parts in MEMS Lidars are able to not only improve the reliability, but also scan a relatively large FOV. The collimated beam utilized in mechanical spinning Lidars, MEMS Lidars and Risley prism systems concentrates the transmitted power and thus increases the detection range. Instead, owing to the divergence of beams the detection range of flash Lidars is limited. Meanwhile, the use of low-density detector arrays reduces the angular resolution of flash Lidars likewise. Hence it is often used to detect large targets at a close range. OPA scanning method is a solution to solidify Lidar systems. However, the optical efficiency of the liquid crystal components has to be improved to further magnify the FOV. According to the discussion in chapter V, Lidar systems with a 1550 nm wavelength benefit to fulfil the requirement of laser safety. Regarding the available commercial systems, the 1550 nm wavelength is only available in MEMS Lidars. Hence, their laser safety is better than other Lidar systems.

VI. CONCLUSIONS

In this paper, the important metrics that influence the performance of Lidar sensors are introduced and investigated. A technical evaluation of different Lidar systems is developed based on the reviews of different commercial systems and the discussion of Lidar metrics. According to the discussion in chapter V, Lidar systems with a pulse modulation and a 1550 nm wavelength are able to maximize the output power and the robustness against the extreme weathers conditions. Meanwhile, compared to 905 nm, Lidar systems with 1550 nm are more tolerant to the requirement of laser safety. According to the Table V, MEMS Lidars are the best comprehensive performance systems. Flash Lidars are pure solid state hence have a good reliability. However, the divergent laser output and sparse detector pixels lead to a lack of their detection range and resolution. Hereafter, the use of 1550 nm laser sources and the increase of the number of the detector pixels can bridge the gap between Flash Lidars and scanning Lidars.

ACKNOWLEDGEMENTS

This work is funded by the Deutsche Forschungsgemeinschaft (DFG, German Research Foundation) under Germany's Excellence Strategy within the Cluster of Excellence PhoenixD (EXC 2122, Project ID 390833453).

REFERENCES

[1] C. Rablau, "LIDAR–A new (self-driving) vehicle for introducing optics to broader engineering and non-engineering audiences," Education and Training in Optics and Photonics, Optical Society of America, May.2019, pp. 11143-138.

[2] R. Halterman and M. Bruch, "Velodyne HDL-64E lidar for unmanned surface vehicle obstacle detection," Proc. SPIE 7692, Unmanned Systems Technology XII, 76920D, May 2010, doi: 10.1117/12.850611.

[3] UNECE Vehicle Regulation 8: Uniform provisions concerning the approval of motor vehicle headlamps emitting an asymmetrical passing beam or a driving beam or both and equipped with halogen filament lamps (H1, H2,.H3, HB3, HB4, H7, H8, H9, H1R1, H1R2 and / or H11). United Nations Economic Commission for Europe, 2012.

[4] UNECE Vehicle Regulation 112: Uniform provisions concerning the approval of motor vehicle headlamps emitting an asymmetrical passing beam or a driving beam or both and equipped with filament lamps and / or light-emitting diode (LED) modules. United Nations Economic Commission for Europe, 2013.

[5] A. Ziebinski, R. Cupek, D. Grzechca and L. Chruszczyk, "Review of advanced driver assistance systems (ADAS)," AIP Conference Proceedings, vol. 1906. No. 1. AIP Publishing LLC, 2017, doi: 10.1063/1.5012394.

[6] SAE On-Road Automated Vehicle Standards Committee. Taxonomy and definitions for terms related to on-road motor vehicle automated driving systems. SAE Standard J, 2014, 3016: 1–16.

[7] A. Lindgren and F. Chen, "State of the art analysis: An overview of advanced driver assistance systems (ADAS) and possible human factors issues," Human factors and economics aspects on safety 38, 2006, pp. 38-50.

[8] A. Carullo and M. Parvis, "An ultrasonic sensor for distance measurement in automotive applications," IEEE Sensors journal 1.2, 2001, pp.143.

[9] A. Bergua, "Elektromagnetisches Spektrum," Das menschliche Auge in Zahlen. Springer, Berlin, Heidelberg, 2017, pp. 173-175, doi: 10.1007/978-3-662-47284-2_36.

[10] S. Liu, J. Tang, Z. Zhang and J. Gaudiot, "Computer Architectures for Autonomous Driving," in Computer, vol. 50, no. 8, 2017, pp. 18-25, doi: 10.1109/MC.2017.3001256.

[11] N. Waltham, "CCD and CMOS sensors." Observing photons in space. Springer, New York, NY, 2013, pp. 423-442.

[12] K. Banerjee, D. Notz, J. Windelen, S. Gavarraju and M. He, "Online Camera LiDAR Fusion and Object Detection on Hybrid Data for Autonomous Driving," 2018 IEEE Intelligent Vehicles Symposium (IV), Changshu, China, 2018, pp. 1632-1638, doi: 10.1109/IVS.2018.8500699.

[13] H. Rashed, M. Ramzy, V. Vaquero, A. El Sallab,G. Sistu, and S. Yogamani, "Fusemodnet: Real-time camera and lidar based moving object detection for robust low-light autonomous driving," Proceedings of the IEEE/CVF International Conference on Computer Vision Workshops, 2019, pp.0-0.

[14] R. H. Rasshofer and K. Gresser, "Automotive radar and lidar systems for next generation driver assistance functions," Advances in Radio Science 3.B. 4, 2005, pp. 205-209.

[15] M. Schneider, "Automotive radar-status and trends," German microwave conference, 2005, pp. 144-147.

[16] J. Hasch, E. Topak, R. Schnabel, T. Zwick, R. Weigel and C. Waldschmidt, "Millimeter-Wave Technology for Automotive Radar Sensors in the 77 GHz Frequency Band," in IEEE Transactions on Microwave Theory and Techniques, vol. 60, no. 3, pp. 845-860, March 2012, doi: 10.1109/TMTT.2011.2178427.

[17] T. Tille, Automobil-Sensorik. Springer Vieweg, 2016, pp. 29-54, doi: 10.1007/978-3-662-48944-4.

[18] I. Vornicu, R. Carmona-Galán and A. Rodríguez-Vázquez, "Photon counting and direct ToF camera prototype based on CMOS SPADs," 2017 IEEE International Symposium on Circuits and Systems (ISCAS), 2017, pp. 1-4, doi: 10.1109/ISCAS.2017.8050410.

[19] S. Bellisai, L. Ferretti, F. Villa, A. Ruggeri, S. Tisa, A. Tosi and F. Zappa, "Low-power 20-meter 3D ranging SPAD camera based on continuous-wave indirect time-of-flight," Proc. SPIE 8375, Advanced Photon Counting Techniques VI, 83750E, May 2012, doi: 10.1117/12.920407.

[20] J. Zhang and S Singh, "LOAM: Lidar Odometry and Mapping in Real-time," Robotics: Science and Systems, vol. 2. No. 9, 2014.

[21] Z. Chen, J. Zhang and D. Tao, "Progressive LiDAR adaptation for road detection," in IEEE/CAA Journal of Automatica Sinica, vol. 6, no. 3, pp. 693-702, May 2019, doi: 10.1109/JAS.2019.1911459.

[22] V. C. Coffey, "Integrated Lidar: Transforming Transportation," Optics and Photonics News 30.9, 2019, pp. 40-47.

[23] Lasertel A Leonardo Company, "The Race to Starting Line: Edge-Emitting Diode Laser vs. VCSELs for the Automotive Lidar Market", White paper, https://www.leonardo.us/edge-emitting-diode-lasers-vs-vcsels-for-the-automotive-lidar-market.

[24] J. Skidmore, "Semiconductor lasers for 3-D sensing," Optics and Photonics News 30.2, 2019, pp. 26-33.

[25] First Sensor, " Making sense of sensors, A LiDAR designer's guide to sensor technologies for automotive/mobility systems", White paper, https://www.first-sensor.com/cms/upload/documentation/2018_White_Paper_Making_Sensor_of_Sensors_LIDAR.pdf.

[26] D. Wang,W. Connor, and H. Xie, "MEMS mirrors for LiDAR: a review," Micromachines 11.5, 2020, pp. 456.

[27] T. Raj, F. H. Hashim, Huddin, A. B., Ibrahim, M. F.,and A. Hussain, "A Survey on LiDAR Scanning Mechanisms," Electronics 9.5, 2020, pp. 741.

[28] C. Pulikkaseril and S. Lam, "Laser eyes for driverless cars: the road to automotive LIDAR," in Optical Fiber Communication Conference (OFC) 2019, OSA Technical Digest, Optical Society of America, 2019, pp. Tu3D.2, doi: 10.1364/OFC.2019.Tu3D.2.

[29] P. McManamon, Field Guide to Lidar, Society of Photo-Optical Instrumentation Engineers (SPIE), Bellingham, Bellingham, 2015.

[30] B. Behroozpour, P. A. M. Sandborn, M. C. Wu and B. E. Boser, "Lidar System Architectures and Circuits," in IEEE Communications Magazine, vol. 55, no. 10, pp. 135-142, Oct. 2017, doi: 10.1109/MCOM.2017.1700030.

[31] H. Zheng, R. Ma, M. Liu and Z. Zhu, "A Linear-Array Receiver Analog Front-End Circuit for Rotating Scanner LiDAR Application," in IEEE Sensors Journal, vol. 19, no. 13, pp. 5053-5061, 1 July1, 2019, doi: 10.1109/JSEN.2019.2905267.

[32] S. G. Kim, S. Jung, X. Ying, H. Choi, Y. S. Eo and S. M. Park, "A 1.8Gb/s/ch 10mW/ch −23dB crosstalk eight-channel transimpedance amplifier array for LADAR systems," 2013 International SoC Design Conference (ISOCC), Busan, Korea (South), 2013, pp. 115-118, doi: 10.1109/ISOCC.2013.6864000.

[33] R. Thakur, "Scanning LIDAR in Advanced Driver Assistance Systems and Beyond: Building a road map for next-generation LIDAR technology," in IEEE Consumer Electronics Magazine, vol. 5, no. 3, pp. 48-54, July 2016, doi: 10.1109/MCE.2016.2556878.

[34] IEC 60825-1: Safety of laser products – part 1: equipment claasification and, requirements. International standar, 2014.

[35] G. Kloppenburg, A. Wolf, R. Lachmayer, "High-resolution vehicle headlamps: technologies and scanning prototype," Adv. Opt. Techn. 2016; 5(2): 147–155

[36] G. Kloppenburg, "Scannende Laser-Projektionseinheit für die Fahrzeugfrontbeleuchtung," PZH Verlag, 2017

[37] M. Knöchelmann, G. Kloppenburg, R. Lachmayer, "Headlamp innovations: optical concepts for fully adaptive light distributions," Proc. SPIE 10546, Emerging Digital Micromirror Device Based Systems and Applications X, 105460K, Feb. 2018, doi:10.1117/12.2290013.

[38] A. Wolf, G. Kloppenburg, R. Danov and R. Lachmayer, "DMD based automotive lighting unit," DGaO Proceedings 2016

[39] B. Smith, B. Hellman, A. Gin, A. Espinoza, and Y. Takashima, "Single chip lidar with discrete beam steering by digital micromirror device," Opt. Express 25, 2017, pp. 14732-14745, doi: 10.1364/OE.25.014732.

[40] H. Schröder, R. Danov, "Time-sequential phase only sub holograms," Proc. SPIE 11698, Emerging Digital Micromirror Device Based Systems and Applications XIII, 116980P, March 2021, doi: 10.1117/12.2584321.

[41] G. F. Marshall, "Risley prism scan patterns," Proc. SPIE 3787, Optical Scanning: Design and Application, July 1999, doi: 10.1117/12.351658.

[42] Z. Liu, F. Zhang and X. Hong, "Low-cost Retina-like Robotic Lidars Based on Incommensurable Scanning," in IEEE/ASME Transactions on Mechatronics, doi: 10.1109/TMECH.2021.3058173.

[43] B. Eberle, T. Kern, M. Hammer, U. Schwanke and H. Nowak, "Novel eye-safe line scanning 3D laser-radar," Proc. SPIE 9249, Electro-Optical and Infrared Systems: Technology and Applications XI, 92490H, October 2014, doi:10.1117/12.2072265.

[44] S. Kameyama, A. Hirai, M. Imaki, N. Kotake, H. Tsuji, Y. Nishino, Y. Ito, M. Takabayashi, Y. Tamagawa, M. Nakaji, E. Ishimura and Y. Hirano, "Demonstration on range imaging of 256×256 pixels and 30 frames per second using short wavelength infrared pulsed time-of-flight laser sensor with linear array receiver," Opt. Eng. 56(3) 031214, November 2016, doi:10.1117/1.OE.56.3.031214.

[45] C. Glennie and D. D. Lichti, "Static calibration and analysis of the Velodyne HDL-64E S2 for high accuracy mobile scanning," Remote sensing 2.6, 2010, pp. 1610-1624.

[46] P. F. McManamon, P. S. Banks, J. D. Beck, D. G. Fried, A. S. Huntington and E. A. Watson, "Comparison of flash lidar detector options," Opt. Eng. 56(3) 031223, March 2017, doi:10.1117/1.OE.56.3.031223.

[47] A. Gelbart, B. C. Redman, R. S. Light, C. A. Schwartzlow, A. J. Griffis, "Flash lidar based on multiple-slit streak tube imaging lidar," Proc. SPIE 4723, Laser Radar Technology and Applications VII, July 2002, doi:10.1117/12.476407.

[48] R. Stettner, "Compact 3D flash lidar video cameras and applications," Proc. SPIE 7684, Laser Radar Technology and Applications XV, 768405, May 2010, doi:10.1117/12.851831.

[49] P. F. McManamon, T. A. Dorschner, D. L. Corkum, L. J. Friedman, D. S. Hobbs, M. Holz and E. A. Watson, "Optical phased array technology," in Proceedings of the IEEE, vol. 84, no. 2, pp. 268-298, Feb. 1996, doi: 10.1109/5.482231.

[50] C. P. Hsu, B. Li, B. S. Rivas, A. Gohil, P. H. Chan, A. D. Moore and V. Donzella, "A Review and Perspective on Optical Phased Array for Automotive LiDAR," in IEEE Journal of Selected Topics in Quantum Electronics, vol. 27, no. 1, pp. 1-16, Jan.-Feb. 2021, Art no. 8300416, doi: 10.1109/JSTQE.2020.3022948.

[51] D. P. Resler, D. S. Hobbs, R. C. Sharp, L. J. Friedman and T. A. Dorschner, "High-efficiency liquid-crystal optical phased-array beam steering," Optics letters 21.9, 1996, pp. 689-691.

[52] Y. Takashima and B. Hellman. "imaging lidar by digital micromirror device," Optical Review, 2020, pp. 1-9.

[53] V. E. Zuev, "Laser-light transmission through the atmosphere," Laser Monitoring of the Atmosphere. Springer, Berlin, Heidelberg, 1976, pp. 29-69.

[54] L. S. Rothman, I. E. Gordon, Y. Babikov, A. Barbe, D. C. Benner, P. F. Bernath and G. Wagner, "The HITRAN2012 molecular spectroscopic database," Journal of Quantitative Spectroscopy and Radiative Transfer 130, 2013, pp. 4-50.

[55] B. Weatherhead, A. Tanskanen, A. Stevermer, S. B. Andersen, A. Arola, J. Austin and D. Tarasick, "Ozone and ultraviolet radiation," 2005, pp. 151-182, ISBN: 13-978-0-521-86509-8.

[56] H. Weichel, Laser beam propagation in the atmosphere. vol. 10319, SPIE press, 1990.

[57] E. J. McCartney, "Optics of the atmosphere: scattering by molecules and particles," New York, 1976.

[58] J. M. Wallace and P. V. Hobbs, "Atmospheric Science: An Introductory Survey Academic Press," New York 467, 1977.

[59] W. E. K. Middleton, Vision through the atmosphere, University of Toronto Press, 1952.

[60] I. I. Kim, B. McArthur and E. J. Korevaar, "Comparison of laser beam propagation at 785 nm and 1550 nm in fog and haze for optical wireless communications," Proc. SPIE 4214, Optical Wireless Communications III, February 2001, doi:10.1117/12.417512.